

Mass-Transported GaInAsP/InP Lasers

A new microfabrication technique, mass transport, has made possible the development of a new breed of semiconductor laser devices. Mass-transported buried-heterostructure GaInAsP lasers are ideally suited for application in optical-fiber communication systems. In fact, the technology for mass-transported buried-heterostructure lasers has been transferred to a commercial fabricator, and these lasers are now being incorporated in optical-fiber communication systems. Mass transport has also led to the first practical surface-emitting diode lasers and monolithic two-dimensional laser arrays. These devices are potentially useful for applications in communications, sensors, optical signal processing, optical computing, and efficient high-power lasers.

Mass transport has been used since 1982 to fabricate a variety of GaInAsP laser devices [1-15]. The mass-transport fabrication technique, described in the box, "Mass Transport," uses surface energy to shape materials into devices to produce lasers with the following properties:

- 1) Low-threshold current
- 2) Good output power and efficiency
- 3) High-speed modulation capability
- 4) High reliability
- 5) Single-frequency emission.

The dominant application for mass-transported lasers, now commercially available, is in optical-fiber communication systems, but future possibilities include free-space communications, optical-fiber sensors, sources for optical signal processing and computing, and optical-fiber links for RF analog signals.

This article describes the fabrication of mass-transported GaInAsP/InP lasers and their optimization for power and speed. It explains why GaInAsP lasers are capable of offering all of the above properties. Finally, the article describes the use of mass transport for fabricating mirrors and beam deflectors, and for integrating optical elements with buried-heterostructure lasers in monolithic systems.

Fabrication of Buried-Heterostructure Lasers

The fundamental structure of the mass-transported GaInAsP laser is a buried heterostructure (BH) fabricated in a planar double-heterostructure (DH) wafer. The use of these structures to define the active (gain) media of diode lasers is discussed and illustrated in the box, "Semiconductor Lasers."

Mass transport provides a simple, easily controlled, and high-yield procedure for making BH lasers in the GaInAsP alloy system [1-6]. Mass-transported BH lasers have a thin strip of a GaInAsP active layer that is totally surrounded by a long narrow mesa of InP. This laser differs radically from conventional diode lasers and provides many advantages, including low threshold current, high-speed modulation capability, and fabrication simplicity. Furthermore, the mass-transport BH design greatly simplifies the manufacture of distributed-feedback (DFB) lasers for single-frequency operation [14].

In the first step of the mass-transport fabrication technique, a planar p-InP/GaInAsP/n-InP DH wafer is grown on an InP substrate. A thin oxide (~2000 Å) is deposited on the epitaxially grown layers. Striped patterns are formed in photoresist by photolithography and then in the oxide (by etching away portions of the oxide).

Mass Transport

Mass transport is a material-migration effect that occurs on compound semiconductors during heat treatment. Etched mesa structures undergo drastic morphological changes in a process of surface-energy minimization (Figs. A and B). First observed on InP [1] and GaAs [2] in 1982, mass transport has been observed on compound semiconductors in general. Recent theoretical modeling and experimental studies show that mass transport is a form of surface diffusion. Similar phenomena exhibited by metals were studied around 1960.

In addition to the BH lasers and integrated mirror facets described in this article, mass

transport can be used (Fig. B) to form high-quality and high-precision microlenses [3] and spherical mirrors that are suitable for monolithic integration with diode lasers and other semiconductor optoelectronic devices.

The first practical surface-emitting diode laser and monolithic two-dimensional laser array were built with the mass-transport technique. Large-scale integration of mass-transported beam deflectors, mirrors, and lenses with lasers, detectors, waveguides, and other optoelectronic elements may lead to optical computers, optical interconnections for VLSI systems, and large coherent 2-D laser arrays.

References

1. Z.L. Liau and J.N. Walpole, "A Novel Technique for GaInAsP/InP Buried Heterostructure Laser Fabrication," *Appl. Phys. Lett.* **40**, 568 (1982).
2. M. Ayabe, H. Nagasawa, and K. Kaneko, "Vapor-Phase Transport of GaAs in V-Shape Grooved GaAs Substrate," *J. Cryst. Growth* **58**, 180 (1982).
3. Z.L. Liau, V. Diadiuk, J.N. Walpole, and D.E. Mull, "Large-Numerical-Aperture InP Lenslets by Mass Transport," *Appl. Phys. Lett.* **52**, 1859 (1988).

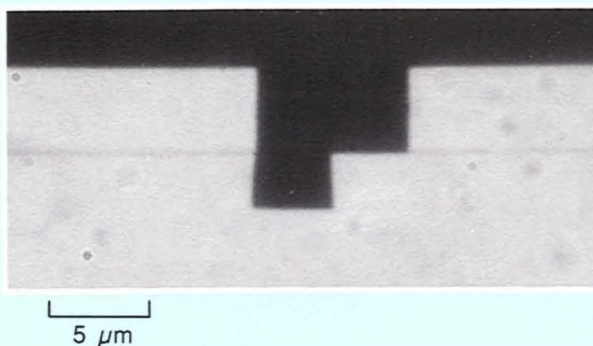
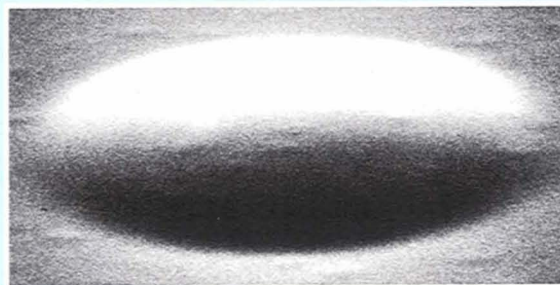


Fig. A — Formation of miniature mirrors by mass transport. The upper photograph shows a stair-shape structure etched in a GaInAsP/InP double-heterostructure wafer. The lower photograph shows smooth mirrors, vertical (left) and 45° (right), formed after mass transport at approximately 730°C.



Etched Mesa Structure



After Mass Transport

Fig. B — Gallium phosphide microlens formation. Semiconductor lenses like this one may permit mass-transported devices to be used in beam-combining systems and other optical-integration applications.

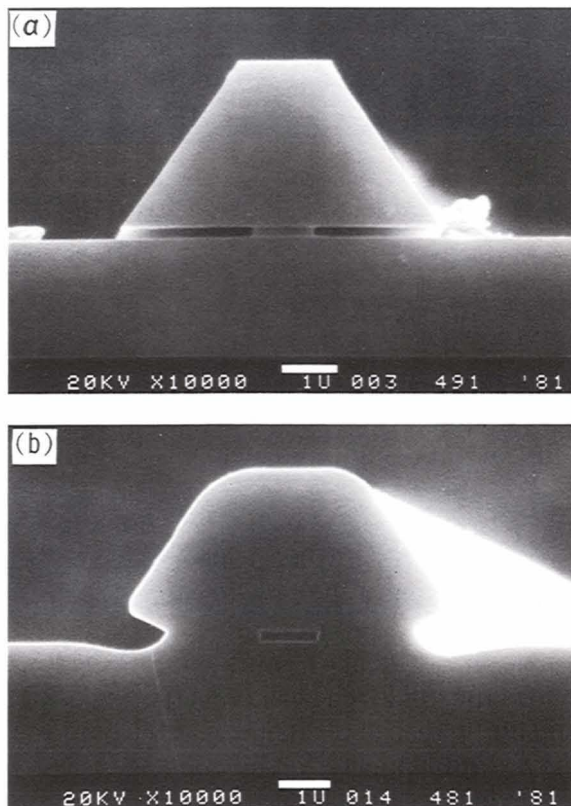


Fig. 1 — (a) Transverse cross section of the etched mesa used in the production of buried heterostructure lasers. The active layer, only 1 μm wide, is not buried. (b) After mass transport at 670°C, the undercut region of the mesa has been buried.

The stripes, a few microns wide, are then used as a mask to etch mesas in the top InP cladding layer. The etchant selectively etches InP and the process stops when the GaInAsP active layer is reached. An etchant that selectively etches GaInAsP is used next and that layer is removed, except under the mesas. However, the etching process does partially undercut the mesas. Figure 1(a) is a scanning electron microscope (SEM) photograph that shows a transverse cross section of such a mesa as it appears after completion of the etching process and removal of the oxide mask. Only a small (approximately 1 μm wide) stripe of the GaInAsP layer remains below the mesa.

At this point, mass transport is used to bury (completely surround with InP) the active GaInAsP layer. Figure 1(b) shows a similar mesa

(somewhat wider at the top than the mesa in Fig. 1[a]) after mass transport. The sharp corners of the mesa are smoothed and the undercut region is largely filled in.

The filled-in (regrown) InP provides edge passivation for the GaInAsP active layers and also completes the waveguide structure, which permits lasing from only one stable lateral mode. The mesa structure also greatly restricts the current (from flowing outside the active region) and minimizes the parasitic capacitance. Therefore, the mass-transported mesa structure is ideally suited for BH laser application. Mass transport is also unique because all other processes used for burying active stripes require epitaxial regrowth over etched nonplanar surfaces [16, 17]. The morphology of regrowth is often difficult to control and, consequently, the yield of useful devices obtained with the regrowth process tends to be low. In addition, the epitaxial regrowth results in large-area current-blocking junctions that greatly increase the parasitic capacitance and severely limit the modulation bandwidth.

To complete the laser fabrication process, the wafer is again coated with a thin ($\sim 2000 \text{ \AA}$) oxide. This time the oxide is patterned with striped openings on top of the mesas. Ohmic contacts (resistivity as low as $10^{-5} \Omega \text{ cm}^2$) are formed through the oxide openings on the tops of the mesas. The substrate side of the wafer is ground to a thickness of about 100 μm (so the wafer can be easily cleaved). An electrical contact is then formed to this side of the wafer. The wafer is cleaved perpendicularly to the mesas into a dozen or so bars. Each bar has approximately 20 lasers. The cleaved facets of the mesas serve as the laser mirrors. Individual lasers are then sawed from the bars. Finally, as shown in the box, "Semiconductor Lasers," the devices are packaged and electrically bonded.

Threshold Currents

Mass transport is a simple fabrication process and it produces lasers that have very low threshold currents. The threshold current is a fundamental property of all lasers. A laser cannot emit coherent light until a sufficient number of elec-

Semiconductor Lasers

The semiconductor diode (injection) laser is made in a single crystal approximately 0.2 mm in each dimension (Fig. A) that comprises micron or submicron layers of varying compositions and doping levels (Fig. B). The layers are arranged so that electrons and holes are injected into a thin low-bandgap region, which leads to efficient stimulated recombination. The low-bandgap region usually has a higher refractive index than the wide-bandgap cladding regions and therefore acts as a dielectric waveguide and confines the laser light, which again improves the laser efficiency. The feedback needed for laser oscillation is provided by the crystal facets (cleaved or etched), which act as partially reflecting mirrors, or by a grating along the waveguide. Additional waveguiding and carrier-confining structures are also formed in the lateral direction of the laser (Fig. C); these structures limit the number of lasing modes and reduce the operating current.

The first GaAs homojunction diode lasers were developed in 1962 by research groups from

General Electric, IBM, and MIT Lincoln Laboratory. Subsequent development of GaAs/GaAlAs heterostructures (Fig. B) led to room-temperature continuous-wave lasers in 1969 [1]. Since 1969, many advances — stripe geometries, distributed feedback schemes, quantum wells, and increased reliability — have been made. Lasers in other compound semiconductors have been developed and a wide range of emission wavelengths is now available.

The first room-temperature operation of $\text{Ga}_x\text{In}_{1-x}\text{As}_y\text{P}_{1-y}$ alloys lattice-matched to InP was reported by J.J. Hsieh and his co-workers at Lincoln Laboratory in 1976 [2]. The GaInAsP laser diodes emit light at wavelengths of 1.1 to 1.6 μm , the most transparent region of the spectrum for silica fibers.

Because laser diodes are small, efficient, and compatible with solid-state electronics, they are being developed for such applications as optical communications, integrated optics, optical information systems, and printing. GaInAsP/InP lasers are used as transmitters in long-distance

optical cables operating at nearly 1 Gbit/s. GaAs diode lasers are commonly found in compact-disc players and are also used to pump solid-state lasers.

Research in semiconductor lasers continues. One- and two-dimensional coherent arrays, tunable single-frequency sources, quantum-well devices, very short- (visible) and long-wavelength diode lasers, and large-scale optoelectronic-integration devices are being developed. Medical applications, including laser surgery, are being explored. Considerable efforts are also focused on crystal growth (bulk and epitaxy) and on fabrication technology, to develop new devices and to lower the cost of existing ones.

References

1. H.C. Casey, Jr. and M.B. Panish, *Heterostructure Lasers* (Academic, New York, 1978).
2. J.J. Hsieh, "Room-Temperature Operation of GaInAsP/InP Double-Heterostructure Diode Lasers Emitting at 1.1 μm ," *Appl. Phys. Lett.* **28**, 283 (1976).

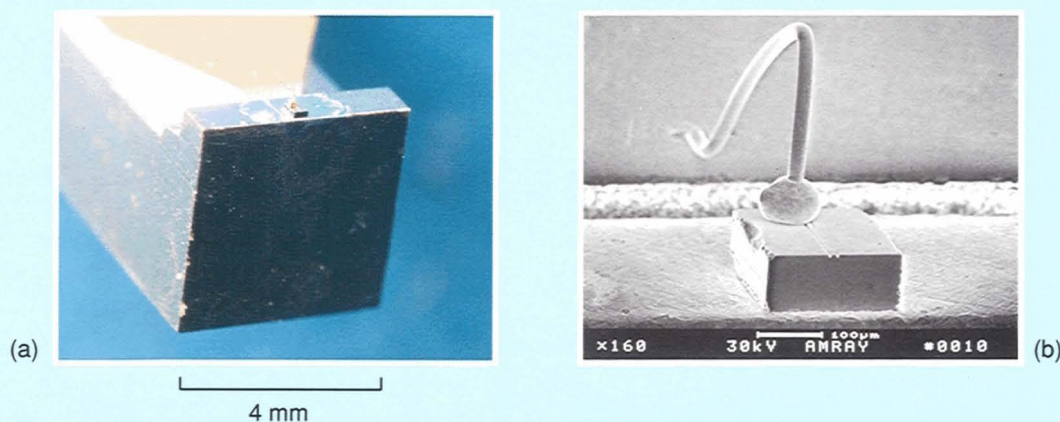


Fig. A — The semiconductor diode laser is a single crystal, about 0.2 mm in each dimension, that appears as a tiny cube mounted on the copper stud shown in the lefthand photograph. The scanning-electron-microscope photograph at the right shows a close-up view of the laser diode. The active region is a very small stripe (approximately 2 μm wide) located under the ridge. An electrical contact is mounted on the ridge.

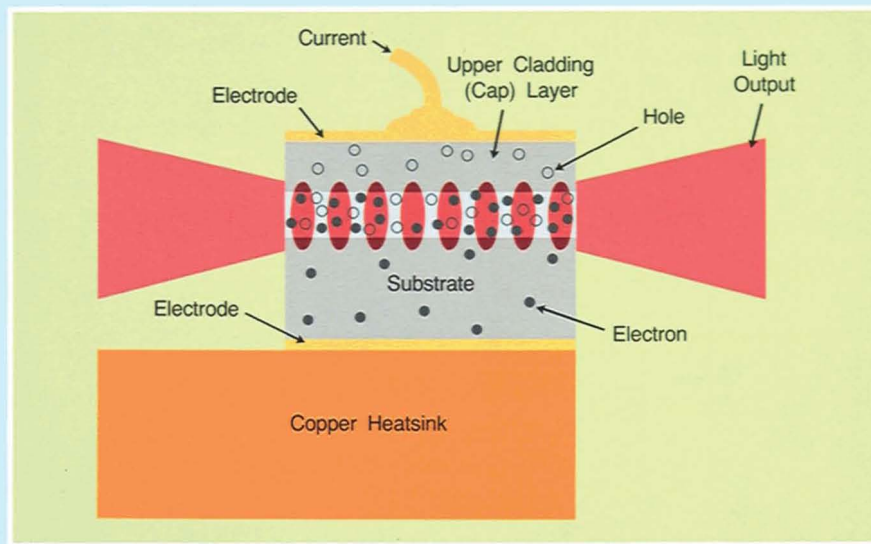


Fig. B—Electrons and holes are injected into the active layer, where they recombine to emit laser light. This longitudinal cross section of a laser diode shows the resonant cavity formed by the two end mirrors (the crystal facets) and the waveguide (the active layer). Note that the lasing mode forms a standing wave along the cavity and that the light penetrates outside the active layer. In an actual device, the active layer is typically $0.1\ \mu\text{m}$ thick and the cavity is 200 to $400\ \mu\text{m}$ long.

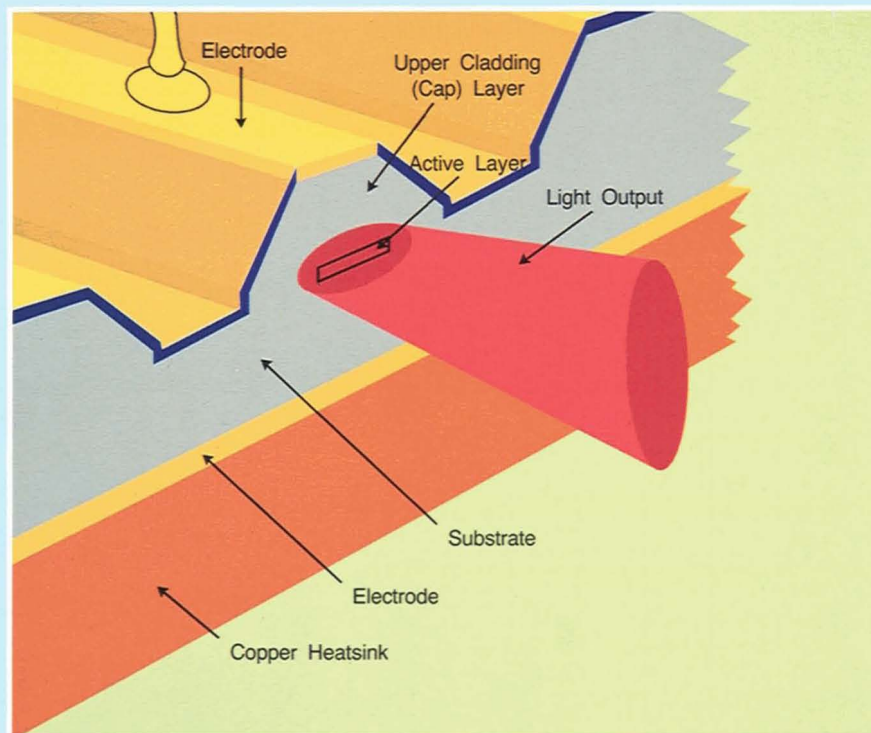


Fig. C — Perspective view of a diode laser. This drawing illustrates the lateral waveguiding and current-confining structures, as well as the output beam. The active layer is typically $2\ \mu\text{m}$ wide.

trons and holes have been injected into its active region and stimulated emission (gain) has overcome the cavity losses. The injected carriers have a lifetime of only 10^{-9} seconds, because they recombine through spontaneous radiative and nonradiative recombination processes. Thus a current must be supplied to maintain the constant carrier concentration in the active region. This current is the threshold current of the laser.

In addition to the electronic band structure and the recombination mechanisms of the active layer, the threshold current depends on such factors as the concentration and type (electrons or holes) of electrical carriers near the active region, which cause free-carrier absorption. Other cavity losses due to waveguide irregularities (scattering of laser light) and low mirror reflectivities can also increase the threshold current. And since lasing action depends on the threshold-current *density*, the volume of the active region can also affect the threshold current.

Low threshold currents are desirable because no useful optical power can be obtained below the threshold. Hence, the electrical power needed to reach the threshold is wasted and increases the requirements for power supplies, laser drivers, and heat-dissipation systems. Low-threshold lasers can be operated with just a few tens of milliwatts of electrical power, a particularly important feature for remote repeaters in a fiber link. Low threshold currents are also important for high-speed modulation.

In typical mass-transported BH lasers, threshold currents are between 10 and 20 mA [1–15]. That figure can be improved (to ~4 to 8 mA) by shrinking the volume of the active region. The power/current plot shown in Fig. 2 was measured for a laser that has about half the volume of the typical GaInAsP laser [18]. The laser's cavity has a length of about $175\text{ }\mu\text{m}$, rather than the more typical $300\text{-}\mu\text{m}$ cavity length, and relatively small transverse dimensions. Its threshold current has been reduced to 4.5 mA, a record low threshold for GaInAsP lasers without facet coating. The gains attainable through reduction of the volume of an active layer are limited, however. As the device be-

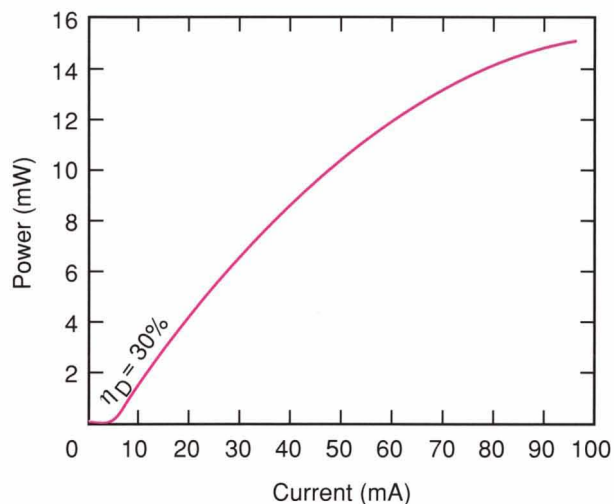


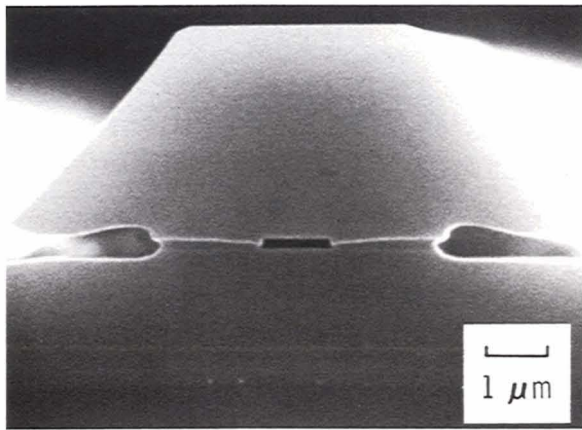
Fig. 2—Output power plotted as a function of drive current. In this reduced-volume device, the threshold current is about 4.5 mA.

comes smaller, the losses become increasingly dominant and the device has to be pumped harder. Eventually, the threshold current actually begins to increase with decreasing volume.

Lower thresholds can also be achieved by applying a high-reflectivity coating (>90% instead of the uncoated facet reflectivity of 30%) to both facets of a laser. With optimized cavity dimensions and facet coatings, threshold currents of 1 to 2 mA may be possible. Since this level of threshold current brings the laser drive current into the range of conventional logic circuits, optical interconnections between electronic circuits could be feasible. Optical interconnection is attractive for the goal of creating denser and faster VLSI circuits.

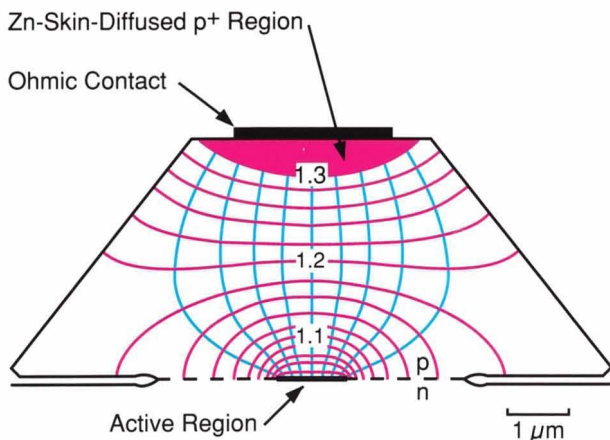
Power and Efficiency

The absorption and scattering losses that contribute to higher threshold currents also determine the differential quantum efficiency of a laser diode. The slope of a power-current curve is directly proportional to the differential quantum efficiency, η_D . The differential quantum efficiency measures the increase in the number of photons obtained from a laser (quanta of optical output power) per electron-hole pair injected into its active layer (quanta of



(a)

Carrier Concentration = $1.0 \times 10^{18} \text{ cm}^{-3}$
 $I = 100 \text{ mA}$



(b) Voltage = 0.0 V in n-InP

Fig. 3 — (a) Scanning electron micrograph of the cleaved cross section of a buried-heterostructure mesa. The device has been stained to reveal the active layer and the p-n junction. The p-n junction extends across the structure in a plane through the active layer. The top cladding layer (cap layer) is p-type; the substrate side of the wafer is n-type. (b) Calculated equipotentials (red) and field lines (blue) for the structure shown in (a).

current drive to the laser).

In Fig. 2, η_D just above the threshold is 30% per facet. Efficiency is normally measured at only one facet. For facets with equal reflectivities, the total efficiency is twice the efficiency per facet. The theoretical maximum output from both facets of a laser is one photon for each

injected electron-hole pair above threshold, but internal losses always prevent attainment of $\eta_D = 100\%$.

In many devices, as the drive current increases well above threshold, η_D decreases. In Fig. 2, for example, η_D decreases from 30% per facet, near threshold, to less than 10% per facet at high current. This sublinearity may be due to an increase in the temperature of a laser's active region. A more common cause, however, is leakage of current around the active region, i.e., current flow through the pair of p-n junctions formed in the transported regions, as shown in the stained cross section in Fig. 3(a). The voltage applied to the device initially causes current to flow predominantly into the active (GaInAsP) region because its energy gap is smaller than that of the adjacent InP junctions. But eventually (at high current), the voltage builds up and the InP junctions are "turned on" and result in current leakage. (The difference in the energy gaps between the active region and the InP region results in a difference in the voltage requirement across the two junction regions to inject similar current densities.) Because of the very simple device geometry, this problem can be analyzed with great accuracy [5].

The calculated current flow (the streamlines) into the active region and the voltage distribution (the equipotentials) in the p-type BH mesa are shown in Fig. 3(b). The voltage along the InP junction (the homojunction) is obtained in this calculation and can in turn be used to evaluate the leakage current. The homojunction leakage current primarily depends on the p-type carrier concentration (because the p-type material is much more resistive than the n-type and is responsible for most of the voltage buildup) and the relative widths of the homojunction region and the active region. A high p-type carrier density and a small homojunction width can limit leakage currents to very small values but may degrade efficiency — by increasing free-carrier absorption and scattering losses, respectively.

Despite these conflicting demands, the p-type carrier density and the homojunction width can be adjusted so that a device can have a low threshold current, high efficiency, and a low

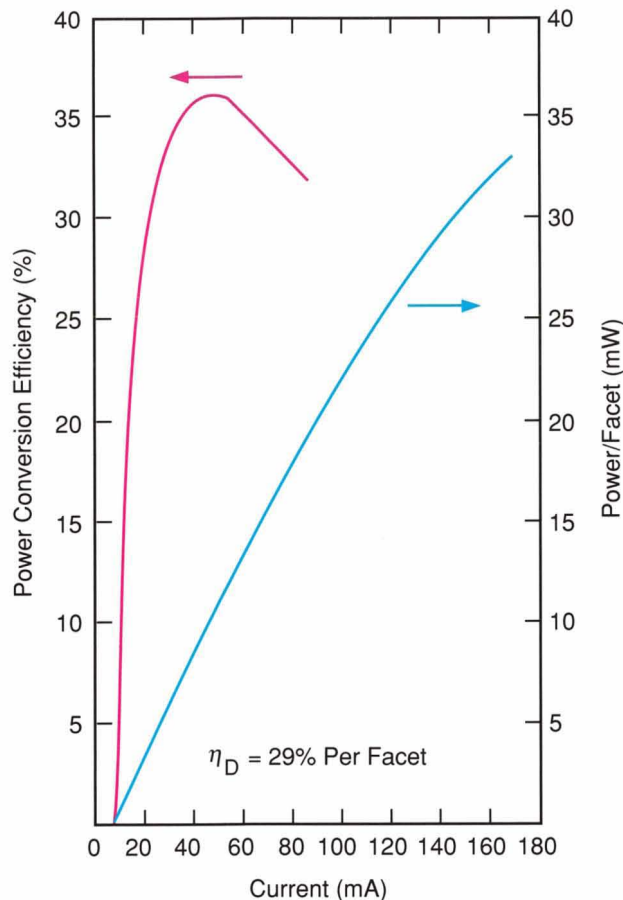


Fig. 4 — Techniques that reduce leakage current tend to reduce efficiency, but a compromise can be struck. These data are taken from a laser that has a very low leakage current. Leakage current increases exponentially with drive current, so output power and drive current generally have a nonlinear relationship. But, up to about 70 mA of drive current, the output power from this device increases linearly with increasing drive current. The device's differential quantum efficiency is approximately 29% per facet.

leakage current [19, 20]. The curves in Fig. 4 illustrate this point. The right vertical axis measures the optical output power per facet; the left vertical axis is the scale for the power conversion efficiency, i.e., the total optical output power divided by the electrical input power. For this laser, the threshold current is 9 mA and the differential quantum efficiency just above threshold is 29% per facet (58% for both facets).

The power conversion efficiency is always lower than the total differential quantum efficiency because the laser threshold current and

the series electrical resistance of the device and its electrical contacts are both greater than zero. But to minimize the power dissipated in series resistance, the laser measured in Fig. 4 was fabricated with a p-type substrate and an n-type cap layer, rather than the opposite polarity, as was discussed earlier and shown in Fig. 3. The p-type contacts are hence formed with the bottom surface of the substrate, rather than with the cap layer. The cap layer has a much smaller contact area than the contact area of the entire substrate because its contact area is just the striped opening in the oxide on the top of the BH mesa. Since the contact resistance of the p-type material is a major part of the series resistance of the device, the larger contacting area of the p-substrate device gives the best series resistance [20]. Contact resistance to the n-type region is usually negligible.

The conversion efficiency of the device in Fig. 4 reaches a maximum just above threshold, then decreases as the fraction of power dissipated in series resistance (proportional to I^2) increases. The maximum efficiency of the device is 36%, including the output from both facets, which is comparable to the highest efficiencies reported for any GaInAsP laser. The very nearly linear dependence of output power on drive current, up to about 70 mA (where the output power from one facet exceeds 15 mW), gives evidence of the device's low leakage current. The low-leakage, high-power capability is also needed for high-speed modulation, because, to have fast responses, the light intensity inside the active layer must be high.

High-Speed Modulation

In communication systems, lasers are usually modulated by direct modulation of the drive current. The mass-transported BH laser is well suited to high-speed modulation because, as just discussed, it can operate at currents many times greater than its threshold current, and yet maintain a low leakage current. The laser's structure permits fabrication, mounting, and packaging that keep the series resistance and the parasitic capacitance and inductance at low levels. And low series resistance, low parasitic

capacitance and inductance, and low leakage current are all absolute requirements for high-speed modulation.

For an ideal laser, with no parasitic elements, the maximum frequency, f_0 , for small-signal sinusoidal modulation is approximately

$$f_0 = \frac{1}{2\pi} \left[\left(\frac{I' - I_{th}}{q} \right) c g' \right]^{1/2} \quad (1)$$

I' is the current injected into the active region (the total current minus any leakage current), I_{th} is the threshold current, q is the electron charge, c is the speed of light inside the laser cavity, and g' is the incremental increase in the laser gain coefficient (measured in cm^{-1}) per injected electron-hole pair. The incremental gain g' is set by the material parameters of the active region and cannot be increased significantly in a simple BH laser. Therefore, large injected current and small threshold current increase the value of f_0 .

Parasitic capacitances are low for the mass-transported BH laser because of the mesa structure. The only inherent parasitic capacitance in the mesa is that due to the homojunction region on each side of the active layer, and this region can be kept very small.

If care is taken to keep the series resistance due to the p-type layer and the ohmic contact small, and if parasitic capacitances and inductances introduced by metallizing, packaging, and bonding are minimized, then the fundamental limit set by Eq. 1 can be reached. Mass-transported BH lasers have demonstrated small-signal modulation (Fig. 5 [a]), with a 3-dB frequency bandwidth of 16.4 GHz [18]. Large-signal digital modulation at 16 Gbit/s (Fig. 5 [b]) has also been measured [18]. Similar results have been reported for BH lasers that were not fabricated with the mass-transport technique, but only if they had the same device geometry as the mass-transported lasers [21–23]. This geometry, called a “constricted mesa,” was first demonstrated by the mass-transport process, but has also been built by using epitaxial regrowth to bury the mesas [21–23]. In practice, however, it may be difficult to prevent mass transport from occurring during epitaxial re-

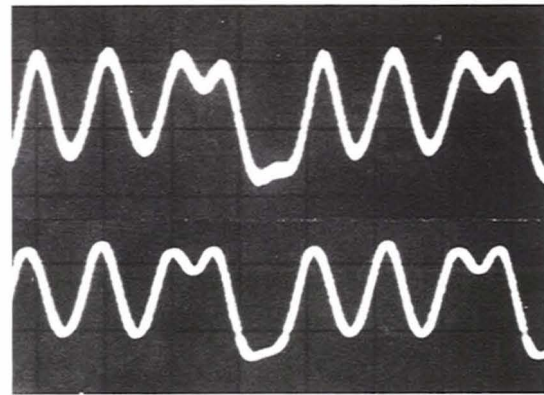
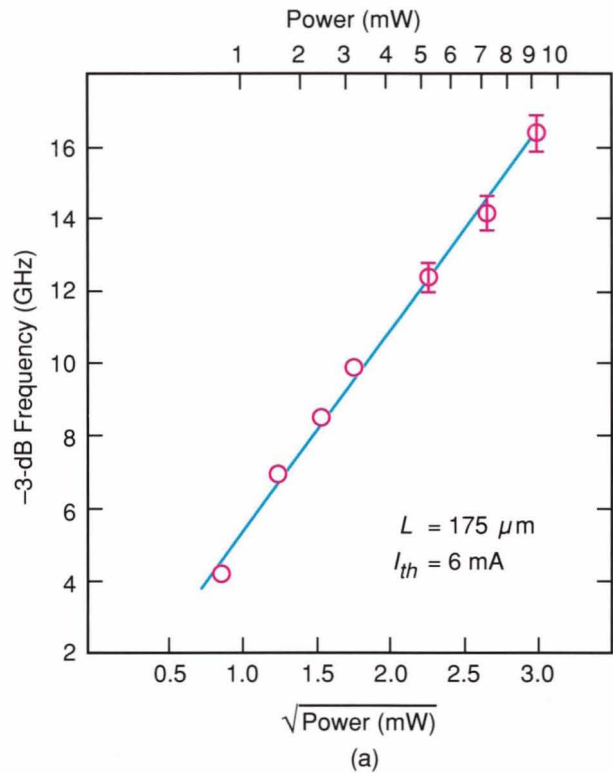


Fig. 5 — (a) Square root of power dependence of modulation bandwidth, in agreement with theory (Eq. 1). (b) High-speed digital modulation of a mass-transported laser at 16 Gbit/s. The top trace corresponds to the detected light signal and the bottom trace corresponds to the electric drive.

growth, so the distinction among the various constricted-mesa geometries may be academic.

Reliability

Good reliability is mandatory for semiconductor lasers, particularly if they will be used for

optical-fiber applications in remote sites. Studies have shown that BH GaInAsP lasers can be made very reliable.

Semiconductor lasers generally have three major device-degradation mechanisms: oxidation of the output facets, catastrophic damage to the output facets, and growth of "dark" regions in the active layer [24].

Oxidation of the output facets due to atmospheric exposure is easily preventable. The facets can be coated with passivating layers of transparent oxides (such as Al_2O_3), which prevent the buildup of the opaque native oxide.

Catastrophic facet damage can destroy other semiconductor lasers, such as AlGaAs lasers, but it is not a problem for GaInAsP lasers. The origin of catastrophic facet damage in an AlGaAs laser is the high nonradiative-recombination rate of electron-hole pairs at the surface of the laser facets. In an AlGaAs laser, recombination depletes the electron-hole population and causes loss (absorption) and intense heating at the facet. This process has not been observed at GaInAsP facets, and does not appear to cause a reliability problem.

The movement and growth of "dark" regions into the active layer of a laser is a serious problem for most semiconductor lasers. Dark regions are regions of crystalline defects that exhibit high nonradiative recombination and don't emit light or provide amplification for the laser. The movement of dark regions into active layers is caused by the propagation of defects originally present in the substrate or introduced by contamination and damage that occur during the growth and processing.

Dark regions grow far more slowly in GaInAsP lasers than in GaAlAs lasers. The most plausible explanation for the slower propagation in GaInAsP comes from the dependence of the propagation rate on the energy gap. The energy required to generate defects for the growth of a dark region must be supplied by recombining electron-hole pairs. The energy of electron-hole pairs is the energy gap of the active medium (plus their thermal energy, ~ 0.026 eV at room temperature). GaAs has an energy gap of 1.43 eV (0.85- μm lasing wavelength); GaInAsP has an energy gap of 0.95 eV (1.3- μm wave-

length). Thus electron-hole pairs have more than 50% as much energy in GaAs than in GaInAsP. Indeed, some of the earliest GaInAsP lasers operated in a continuous-wave (CW) mode for hundreds and even thousands of hours without degradation [25], in sharp contrast to the early development of GaAlAs lasers.

Mass-transported buried-heterostructure lasers have shown little degradation during extended operation at room temperature [26, 27]. Moreover, the operating life of the best commercially available mass-transported BH lasers is currently specified for a median time to failure of 300 years, based on accelerated-aging studies at high temperatures [27]. However, the yield of extremely reliable devices remains low and more studies are needed of material- or fabrication-induced defects.

Single-Frequency Lasers

Most GaInAsP lasers, at least under modulation, radiate in more than one of the longitudinal modes of the laser cavity, and the laser power fluctuates rapidly from mode to mode. The total laser power may be relatively stable, but its distribution is not. The fluctuation of laser power among several modes is called "mode-partition noise."

Mode-partition noise can be a particular problem in long fiber links because of spectral dispersion in optical fibers. Different longitudinal modes emit radiation at slightly different frequencies, and the dispersion of the fiber broadens the signal. Therefore, as short pulses (at a high data rate) pass through a long fiber, mode-partition noise can broaden the pulses beyond acceptable limits. This problem can be eliminated by operating the laser in a single-frequency mode.

Heterodyne-communication systems also require a single-frequency laser, since the laser frequency serves as the carrier and the local oscillator frequency. For low-noise (10^{-9} bit error rate) heterodyne-communication systems, 99% or more of the total power must be in one mode.

Ordinary GaInAsP lasers, with optical cavities defined by a pair of parallel mirrors at each end of the laser medium (Fabry-Perot-cavity lasers),

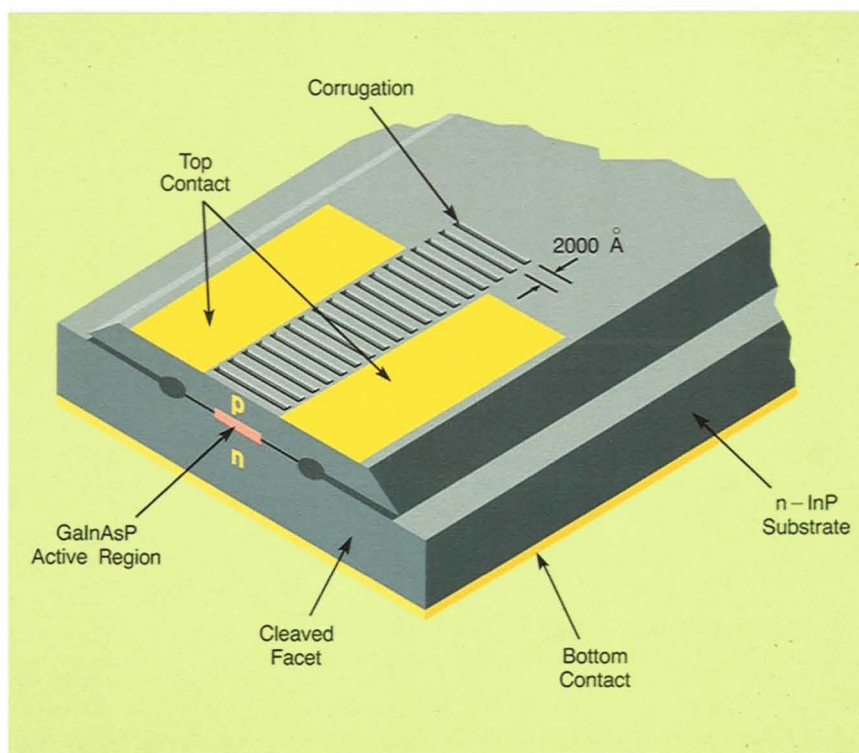


Fig. 6 — A greatly simplified distributed-feedback laser based on the mass-transported buried heterostructure. The grating etched into the top of this mesa is a periodic array of deep rectangular grooves. The periodicity is approximately $0.2\text{ }\mu\text{m}$ and is one-half the wavelength of the $1.3\text{-}\mu\text{m}$ radiation inside the laser cavity with a refractive index of approximately 3.2. From the top of the mesa, the grooves appear as $0.1\text{-}\mu\text{m} \times 2\text{-}\mu\text{m}$ holes that extend into the cap to a depth of about $0.25\text{ }\mu\text{m}$. The thickness of the cap layer is about $1.0\text{ }\mu\text{m}$. The actual device length is $450\text{ }\mu\text{m}$, including a $75\text{-}\mu\text{m}$ unpumped section.

are not capable of single-mode operation under modulation. Greater mode selectivity can be obtained by incorporating a frequency-selective grating in each end of the laser medium (a distributed-Bragg-reflector laser) or along the length of the laser medium (a DFB laser). And mass-transported (BH) lasers are easily fabricated as DFB lasers.

A novel method of producing a DFB laser uses the constricted-mesa shape [14], as shown in Fig. 6. The two openings in the oxide layer along the edges of the mesa top provide electrical contact to the cap layer; these contacts do not extend the full length of the device. At one end of the cavity, an unpumped region absorbs radiation that might otherwise reflect back into the

cavity and produce Fabry-Perot oscillation modes.

A DFB grating has been etched into the middle of the mesa, directly above the active region. The grooves in the grating must be deep enough that the laser-mode index is perturbed by their presence. Coherent addition of reflections will then occur only at selected (relatively few) frequencies. If the threshold for one frequency is much lower than for all other frequencies, the laser will operate in a single mode.

The grating in the DFB structure in Fig. 6 is a periodic array of deep rectangular grooves. Special submicron lithography and etching techniques were required to produce it. The pattern for the grating was generated holo-

graphically and was transferred to an etch mask by using X-ray lithography. The etching technique used was ion-beam-assisted etching, a dry etching technique that can produce a large depth-to-width ratio in the etched grooves.

The DFB grating was fabricated after all the epitaxial layers were deposited. By contrast, in conventional fabrication of grating-coupled devices, the grating is formed at the interface of epitaxial layers of different optical indices [15, 17, 21]. However, it is usually not a good idea to etch into the active layer, so it is necessary to grow an extra layer near the active layer that has an index intermediate between the active layer and the cladding layer. Therefore, an extra layer is required (and the waveguide is complicated). Moreover, an epitaxial layer must be grown over the etched grating, a procedure that often causes uniformity problems and grating deterioration (due to mass transport!). Our approach prevents these problems.

Figure 7 shows the emission spectrum from one of our DFB lasers. The spectrum is dominated by a mode at about $1.31\ \mu\text{m}$. Other structures at the sides of the main mode can be seen, but only when the spectrum is magnified 1,000 times. The largest peaks in the side structure have an intensity of $-32\ \text{dB}$ relative to the main mode, far exceeding the requirement of $-20\ \text{dB}$ (99% of the power in the main mode) specified for single-frequency operation.

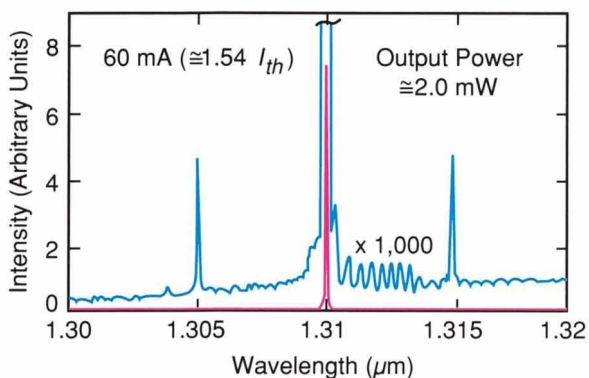


Fig. 7 — The distributed-feedback design has concentrated all power into one mode of this laser. The intensity of the largest peak in the side structure is $-32\ \text{dB}$ from the main mode.

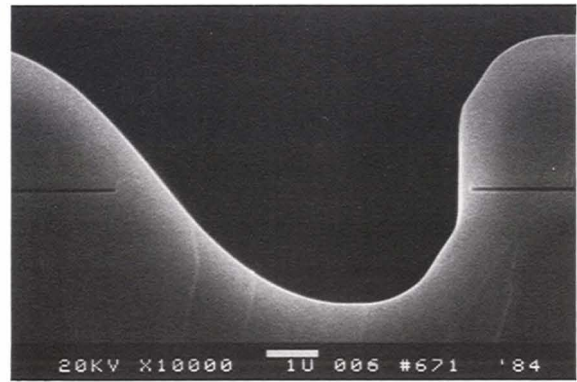


Fig. 8 — Scanning electron micrograph of the longitudinal cross section, near the emission end, of a surface-emitting laser before metallization. The parabolic mirror on the left, which was produced by mass transport, deflects the output of the laser on the right at a right angle to the plane of the laser wafer. The white bar is a $1\text{-}\mu\text{m}$ scale.

The data were obtained at a current of $60\ \text{mA}$ (1.54 times the threshold current). Often, a laser will operate in one mode near its threshold current, but will operate in more than one mode when the drive current is increased to more than 10 to 20% above threshold. The data for Fig. 7 were measured at a drive current that is 50% over threshold to assure that the DFB laser is, indeed, a single-mode laser.

Surface-Emitting Lasers and Monolithic Two-Dimensional Arrays

Mass transport can be used to fabricate a variety of miniature optical components, including mirrors, beam deflectors, and lenses [7–13]. These components can be integrated with mass-transported BH lasers to fabricate surface-emitting lasers (light emission perpendicular to wafer surface) and to create new types of optical and electrooptical systems.

A photograph of a double-heterostructure wafer during fabrication of a surface-emitting laser is presented in the box, “Mass Transport.” Two separate steps of masking and selective chemical etching were required to create the staircase profile. The smooth 45° mirror is the result of performing the mass-transport procedure on the staircase profile. The smooth verti-

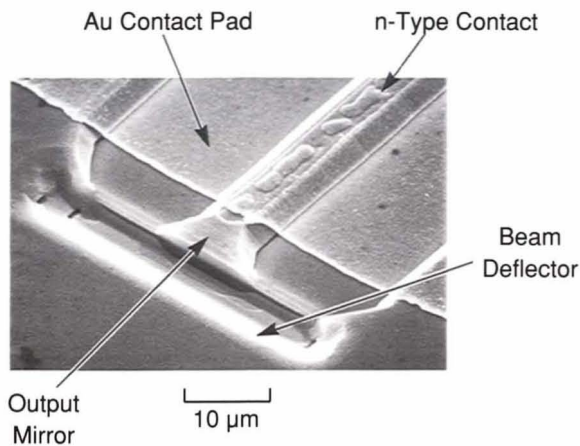


Fig. 9— Scanning electron micrograph showing a perspective view of a surface-emitting laser near its emission end.

cal surface on the other side of the groove is perpendicular to the active region, and provides one of the mirrors required for a Fabry-Perot cavity. Thus the output mirror is obtained without cleaving the wafer, which should greatly enhance yield and uniformity. The 45° mirror can be used to deflect the laser light perpendicularly to the wafer surface. The SEM photograph of Fig. 8, a high-magnification cross-sectional view taken at the completion of mass transport, reveals the smoothness produced by the mass-transport process, which yields high optical quality.

This integrated mirror structure has resulted in the first surface-emitting laser with a performance comparable to the conventional edge-emitting ones [8]. The SEM photograph in Fig. 9 shows one device near its emission end; the infrared micrograph in Fig. 10 shows an array of 16 surface-emitting lasers in operation. These devices easily run CW at room temperature and show low threshold current of only 6 mA and high output power of 30 mW per laser. This performance compares very favorably with other types of surface-emitting lasers currently under development [28, 29] (which use either a vertical cavity or a second-order grating). Surface-emitting lasers are clearly desirable for large-scale monolithic integration, because the conventional cleaving procedure completely limits diode lasers to discrete devices.

Shown in Fig. 10 is the first monolithic two-dimensional laser array ever produced [9]. The development of two-dimensional laser arrays opens up a number of potential applications. These arrays may lead to efficient production of high optical power, because semiconductor lasers are much more efficient than solid-state or gas lasers. But to reach this goal, arrays of thousands of devices, with uniform characteristics, are needed. Fabrication of such arrays presents a considerable challenge to present InP material technology. As a first attempt, millimeter-size arrays containing more than 100 lasers have been fabricated [10].

Figure 11 is a composite of several infrared photographs of a 160-element, 4,000-lasers/cm² array. The light output appears as bright spots, with surface features of the array including some bonding wires in the background. Arrays similar to this one have developed 0.7 W of continuous output power at room temperature and 1.3 W at 11°C. Further improvements in device performance, metallization schemes, and heatsink technology should lead to 1-cm² arrays that deliver more than 100 W.

In many applications, it is desirable that a

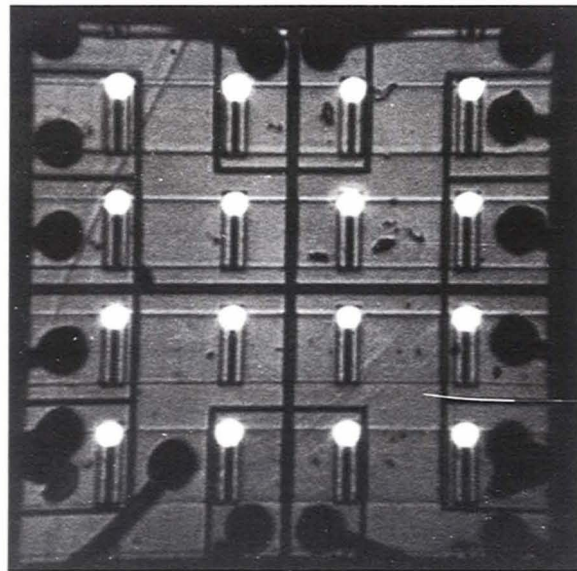
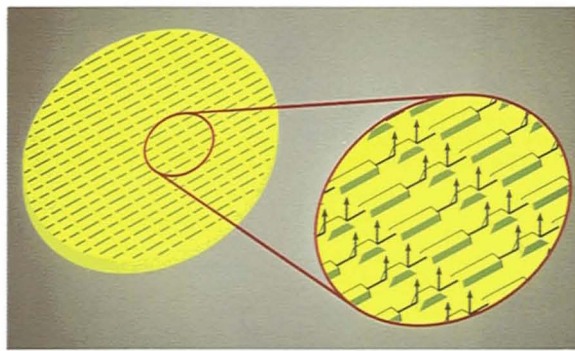


Fig. 10 — Infrared photograph of a monolithic two-dimensional surface-emitting laser array in operation. This is the first monolithic two-dimensional laser array ever produced.



- $\lambda = 1.3 \mu\text{m}$
- 10 mW/Laser/cm^2
- 40 W/cm^2
- 36% Power Efficiency for Individual Elements

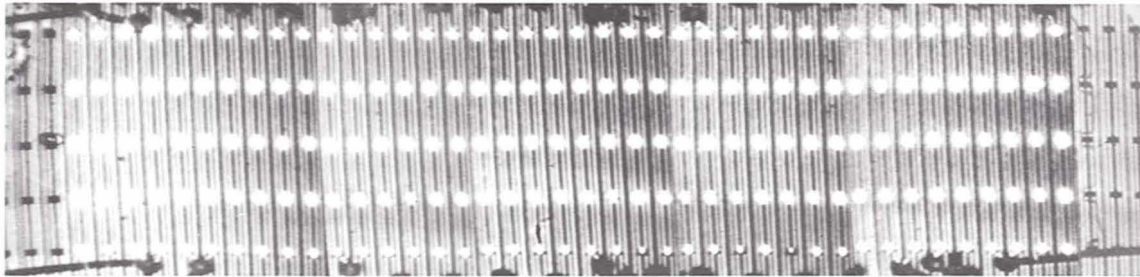


Fig. 11 — A 160-element laser array packed with 4,000 lasers/cm². This figure is a composite of several photographs of an infrared vidicon system's monitor.

large array have a phase-locking scheme that makes the entire array coherent. Several external-cavity phase-locking schemes have been demonstrated on one-dimensional arrays that can be applied to the two-dimensional arrays [30–31]. Implementation of the phase-locking to two-dimensional arrays remains, however, a considerable technical challenge. Meanwhile, much work is being done on coherent one-dimensional arrays that consist of mutually coupled multistripes [13, 32]. This work may lead to useful insights into the problem of phase-locking semiconductor lasers.

Cylindrical Mirrors and Coherent One-Dimensional Laser Arrays

Cylindrical mirrors can be etched at the ends of laser cavities and smoothed by mass transport [11–13]. Since it is clear that curved reflec-

tors can deflect, collimate, and focus optical beams on the surface of a wafer, cylindrical mirrors should be able to facilitate advanced optoelectronic integration in the future.

The entire integrated structure (the buried-heterostructure waveguide gain region and the cylindrical output mirror), shown in Fig. 12, was formed at the same time by ion-beam-assisted etching and mass transport. In addition to providing the feedback, the cylindrical mirror acts as a lens and collimates the output beam in the lateral direction — from a typical divergence of 30° to approximately 10°. When offset halfway between adjacent stripes, the cylindrical mirrors can efficiently couple multiple laser stripes together and form a coherent array [13].

A coupled laser array is shown in Fig. 13. The array of cylindrical mirrors takes a scallop shape. The mirrors focus the output of each waveguide onto its immediate neighbors, thus

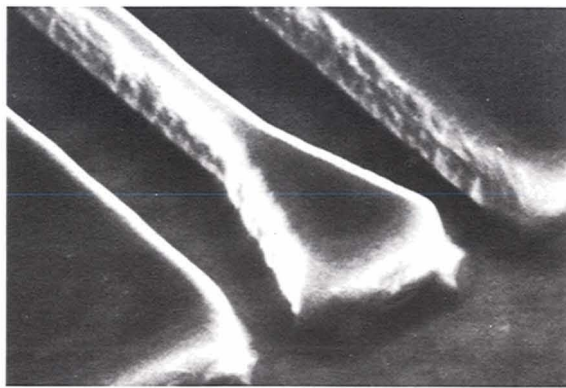


Fig. 12 — Scanning electron micrograph of a buried-heterostructure laser mesa with a cylindrical end mirror.

achieving mutual injection locking and coherent coupling. However, improvements are still needed for stronger and more stable coupling. Furthermore, the close spacing of stripes in these arrays makes heatsinking difficult.

Cylindrical mirrors can also be used for aperture filling the laser-array output [13]. Without aperture filling, a coherent array produces an undesirable multilobe far-field pattern. Narrowing of the far-field pattern to a nearly single lobe has been demonstrated by adding scalloped output mirrors (without an offset) to the laser array.

Conclusions

Current mass-transported buried-heterostructure lasers meet the requirements of fiber-optic communications. All the optical elements required to deflect and focus optical signals can be produced by mass-transport fabrication techniques and future applications will exploit this in the fabrication of mirrors, lenses, and beam deflectors for production of surface-emitting lasers and laser arrays, and for optoelectronic integration. These elements may pave the way for the development of complex integrated optical systems for extremely high-speed com-

puters and communication systems. Other areas for development of mass-transported devices include the monolithic integration of microlens arrays with lasers to produce coherently combined beams.

Mass-transport technology is applicable to materials other than GaInAsP/InP. By applying

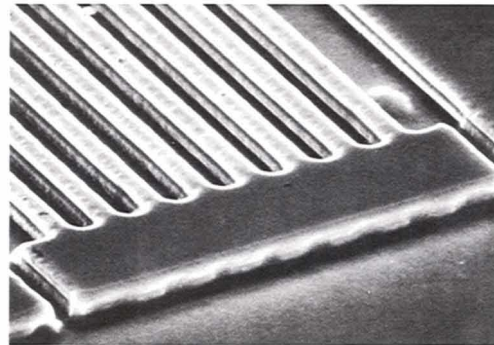


Fig. 13 — Scanning electron micrograph of an array of buried-heterostructure mesa stripes. A scallop mirror in the end region provides for efficient diffraction coupling between stripes.

this fabrication technique to other semiconductor materials, it should be possible to produce optical devices that operate at shorter and longer wavelengths than GaInAsP/InP lasers.

Acknowledgments

The authors wish to acknowledge the work of their collaborators, particularly D.Z. Tsang on low-threshold lasers and high-speed modulation, V. Diadiuk on coherent arrays and microlenses, D. Yap and L.J. Missaggia on cylindrical mirrors, D.E. Mull on wafer growth and mass transport, D.C. Flanders and N.L. DeMeo on DFB lasers, G.W. Iseler on bulk InP growth, P.M. Nitishin on SEM, and H.J. Zeiger on mass-transport modeling. Assistance in epitaxial growth, device fabrication, packaging, and testing has been obtained from G.A. Brigham, S.A. Connor, C.A. Costa, B. DiGiorgio,

D.J. Gingras, G.A. Ferrante, L.P. Hammond, T.A. Lind, W.F. McBride, L.J. Missaggia, and R.D. Sisson. Finally, S.H. Groves, J.J. Hsieh,

F.J. Leonberger, I. Melngailis, D.L. Spears, and R.C. Williamson have provided many stimulating discussions and helpful suggestions.

References

1. Z.L. Liau and J.N. Walpole, "A Novel Technique for GaInAsP/InP Buried Heterostructure Laser Fabrication," *Appl. Phys. Lett.* **40**, 568 (1982); *IEEE Trans. Electron Dev.* **ED-29**, 1675 (1982).
2. T.R. Chen, L.C. Chiu, K.L. Yu, U. Koren, A. Hasson, S. Margalit, and A. Yariv, "Low Threshold InGaAsP Terrace Mass Transport Laser on Semi-Insulating Substrate," *Appl. Phys. Lett.* **41**, 1115 (1982).
3. A. Hasson, L.C. Chiu, T.R. Chen, U. Koren, Z. Rav-Noy, K.L. Yu, S. Margalit, and A. Yariv, "Selective Low-Temperature Mass Transport in InGaAsP/InP Lasers," *Appl. Phys. Lett.* **43**, 403 (1983).
4. Y. Noguchi, Y. Suzuki, T. Matsuoka, and H. Nagai, "InP/InGaAsP p-Type Substrate and Mass Transported Doubly Buried Heterostructure Laser," *Electron Lett.* **20**, 769 (1984).
5. Z.L. Liau, J.N. Walpole, and D.Z. Tsang, "Fabrication, Characterization and Analysis of Mass-Transported GaInAsP/InP Buried-Heterostructure Lasers," *IEEE J. Quantum Electron.* **QE-20**, 855 (1984).
6. D. Yap, Z.L. Liau, D.Z. Tsang, and J.N. Walpole, "High-Performance InGaAsP/InP Buried-Heterostructure Lasers and Arrays Defined by Ion-Beam-Assisted Etching," *Appl. Phys. Lett.* **52**, 1464 (1988).
7. Z.L. Liau, J.N. Walpole, and D.Z. Tsang, "Low-Threshold GaInAsP/InP Buried-Heterostructure Lasers with a Chemically Etched and Mass-Transported Mirror," *Appl. Phys. Lett.* **44**, 945 (1984).
8. Z.L. Liau and J.N. Walpole, "Surface-Emitting GaInAsP/InP Laser with Low-Threshold Current and High Efficiency," *Appl. Phys. Lett.* **46**, 115 (1985).
9. J.N. Walpole and Z.L. Liau, "Monolithic Two-Dimensional Arrays of High-Power GaInAsP/InP Surface-Emitting Lasers," *Appl. Phys. Lett.* **48**, 1636 (1986).
10. Z.L. Liau and J.N. Walpole, "Large Monolithic Two-Dimensional Arrays of GaInAsP/InP Surface-Emitting Diode Lasers," *Appl. Phys. Lett.* **50**, 528 (1987).
11. J.N. Walpole, Z.L. Liau, L.J. Missaggia, and D. Yap, "Diode Lasers with Cylindrical Mirror Facets and Reduced Beam Divergence," *Appl. Phys. Lett.* **50**, 1219 (1987).
12. D. Yap, J.N. Walpole, and Z.L. Liau, "InGaAsP/InP Buried-Heterostructure Lasers with Concurrent Fabrication of the Stripes and Mirrors," *Appl. Phys. Lett.* **53**, 1260 (1988).
13. D. Yap, "Dry-Etched InGaAsP/InP Buried-Heterostructure Lasers and Laser Arrays," Ph.D. Thesis (Massachusetts Institute of Technology, Cambridge, MA, 1988).
14. Z.L. Liau, D.C. Flanders, J.N. Walpole, and N.L. DeMeo, "A Novel GaInAsP/InP Distributed Feedback Laser," *Appl. Phys. Lett.* **46**, 221 (1985).
15. B. Broberg, F. Koyama, Y. Tohmori, and Y. Suematsu, "1.53 μm DFB Lasers by Mass Transport," *Electron. Lett.* **20**, 692 (1984).
16. H. Ishikawa, H. Imai, T. Tanahashi, K. Hori, and K. Takahei, "V-Grooved Substrate Buried-Heterostructure InGaAsP/InP Laser Emitting at 1.3 μm Wavelength," *IEEE J. Quantum Electron.* **QE-18**, 1704 (1982).
17. M. Kitamura, M. Yamaguchi, S. Murata, I. Mito, and K. Kobayashi, "Low-Threshold and High-Temperature Single-Longitudinal-Mode Operation of 1.55 μm -Band DFB-DC-PBH LDs," *Electron. Lett.* **20**, 595 (1984).
18. D.Z. Tsang and Z.L. Liau, "Sinusoidal and Digital High-Speed Modulation of p-Type Substrate Mass-Transported Diode Lasers," *J. Lightwave Technol.* **LT-5**, 300 (1987).
19. Z.L. Liau and J.N. Walpole, "Prevention of Current Leakage in Mass-Transported GaInAsP/InP Buried-Heterostructure Lasers with Narrow Transported Regions," *IEEE J. Quantum Electron.* **QE-23**, 313 (1987).
20. Z.L. Liau, J.N. Walpole, D.Z. Tsang, and V. Diadiuk, "Characterization of Mass-Transported p-Substrate GaInAsP/InP Buried-Heterostructure Lasers with Analytical Solutions for Electrical and Thermal Resistances," *IEEE J. Quantum Electron.* **QE-24**, 36 (1988).
21. T.L. Koch, T.J. Bridges, E.G. Burkhardt, P.J. Corvini, L.A. Coldren, R.A. Linke, W.T. Tsang, R.A. Logan, L.F. Johnson, R.F. Kazarinov, R. Yen, and D.P. Wilt, "1.55- μm InGaAsP Distributed Feedback Vapor-Phase-Transported Buried-Heterostructure Lasers," *Appl. Phys. Lett.* **47**, 12 (1985).
22. C.B. Su, V. Lanzisera, R. Olshansky, W. Powazinik, E. Meland, J. Schlafer, and R.B. Lauer, "15 GHz Direct Modulation Bandwidth of Vapor-Phase-Regrown 1.3 μm InGaAsP Buried-Heterostructure Lasers under CW Operation at Room Temperature," *Electron Lett.* **21**, 577 (1985).
23. J.E. Bowers, "Millimeter-Wave Response of InGaAsP Lasers," *Electron. Lett.* **21**, 1195 (1985).
24. H.C. Casey, Jr. and M.B. Panish, *Heterostructure Lasers* (Academic, New York, 1978).
25. C.C. Shen, J.J. Hsieh, and T.A. Lind, "1500-h Continuous CW Operation of Double-Heterostructure GaInAsP/InP Lasers," *Appl. Phys. Lett.* **30**, 353 (1977).
26. H. Jung, E.G. Burkhardt, and W. Pfister, "Reduction of Degradation in Vapor-Phase-Transported InP/InGaAsP Mushroom Stripe Lasers," *Appl. Phys. Lett.* **53**, 1230 (1988).
27. A. Rosiewicz and W. Rideout, private communication.
28. K. Iga, S. Kinoshita, and F. Koyama, "Recent Advances of Surface-Emitting Semiconductor Lasers," *Optoelectronics—Devices and Technologies* **3**, 131 (1988).
29. G.A. Evans, N.W. Carlson, J.M. Hammer, M. Lurie, J.K. Butler, S.L. Palfrey, R. Amantea, L.A. Carr, F.Z. Hawrylo, E.A. James, C.J. Kaiser, J.B. Kirk, W.F. Reichert, S.R. Chinn, J.R. Sealy, and P.S. Zory, "Coherent, Monolithic Two-Dimensional (10×10) Laser Arrays Using Grating Surface Emission," *Appl. Phys. Lett.* **53**, 2123 (1988).
30. R.H. Rediker, R.P. Schloss, and L.J. Van Ruyven, "Operation of Individual Diode Lasers as a Coherent Ensemble Controlled by a Spatial Filter within an External Cavity," *Appl. Phys. Lett.* **46**, 133 (1985).
31. J.R. Leger, M.L. Scott, and W.B. Veldkamp, "Coherent Addition of AlGaAs Lasers Using Microlenses and Diffractive Coupling," *Appl. Phys. Lett.* **52**, 1771 (1988).
32. D.R. Scifres, R.D. Burnham, and W. Streifer, "High-Power Coupled Multiple Stripe Quantum Well Injection Lasers," *Appl. Phys. Lett.* **41**, 118 (1982).



ZONG-LONG LIAU received a B.S. degree in physics from the National Taiwan University 1972, and a Ph.D. degree in applied physics from the California Institute of Technology in 1979. Since 1978 he has been a staff member in the

Applied Physics Group at Lincoln Laboratory. His work at Lincoln Laboratory has centered on GaInAsP/InP diode lasers and integrated optoelectronics. He has been particularly involved in the development of the mass-transport technique for fabricating buried-heterostructure lasers, distributed-feedback lasers, surface-emitting lasers, lenslets, and monolithic two-dimensional arrays of these structures. Zong-Long has been awarded five U.S. patents.



JAMES N. WALPOLE received a B.S.E.E. degree from Duke University in 1961, and M.S. and Ph.D. degrees in electrical engineering in 1962 and 1966, respectively. In 1966 he was appointed Assistant Professor in the Department of

Electrical Engineering at MIT and became Associate Professor in 1971. Jim wrote his doctoral thesis while working at Lincoln Laboratory and then joined the Laboratory in 1972. He is now a staff member in the Applied Physics Group. His recent research includes the development of GaInAsP lasers, particularly mass-transported buried heterostructures, distributed-feedback lasers, intracavity-loss-modulated (Q-switched) lasers, and lasers with etched and transported mirrors and monolithic integrated beam deflectors for emission from the wafer surface. These last devices are being developed into two-dimensional laser arrays. He holds six U.S. patents.